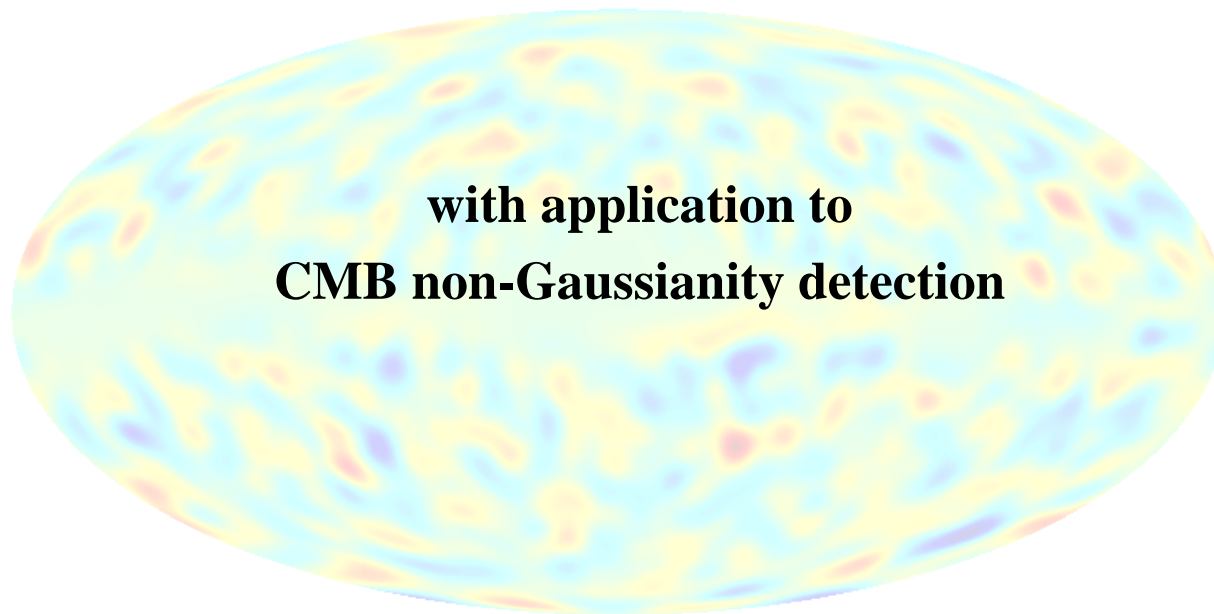


A Fast Directional Spherical Wavelet Transform

for the Analysis of Cosmological Data



Overview

- Directional Continuous Spherical Wavelet Transform (CSWT)
- Fast algorithm
- Deviation from Gaussianity in WMAP anisotropies using spherical wavelet analysis
 - Isotropic spherical Mexhat wavelets
 - Directional spherical real Morlet wavelets
- Conclusions and future work



- Follow the formalisation of Antoine and Vandergheynst (1999)

- Notation

$$S^2, \omega = (\theta, \phi), d\mu(\omega) = \sin(\theta)d\theta d\phi$$

- Rotations

$$(\mathcal{R}_\rho f)(\omega) = f(\rho^{-1}\omega) \quad \text{where } f \in L^2(S^2), \rho \in SO(3)$$



- Dilations

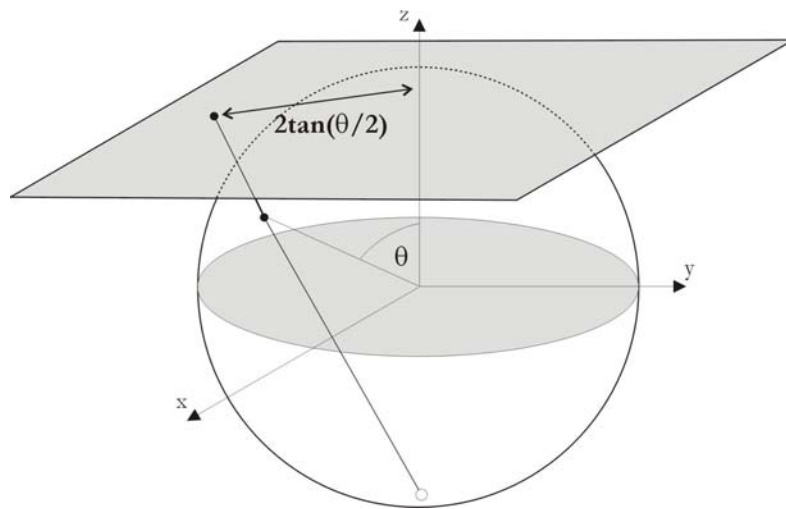
$$(\mathcal{D}_a f)(\omega) = f_a(\omega) = \sqrt{\lambda(a, \theta)} f(\omega_{1/a}), \quad a \in \mathbb{R}_*^+$$

where $\omega_a = (\theta_a, \phi)$,

$$\tan(\theta_a/2) = a \tan(\theta/2)$$

enforce

$$\|\mathcal{D}_a f\|_2 = \|f\|_2 \Rightarrow \lambda(a, \theta)$$



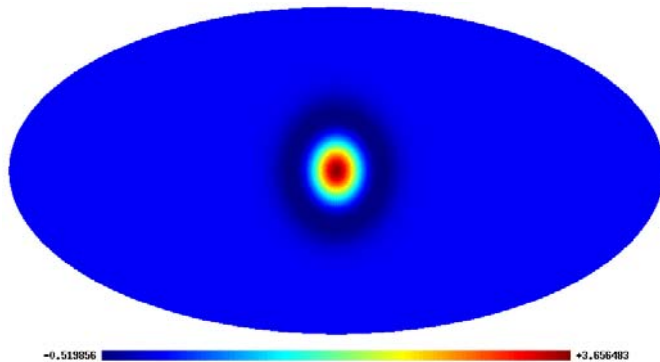
Inverse Stereographic Projection



- Project Euclidean planar wavelets onto the sphere

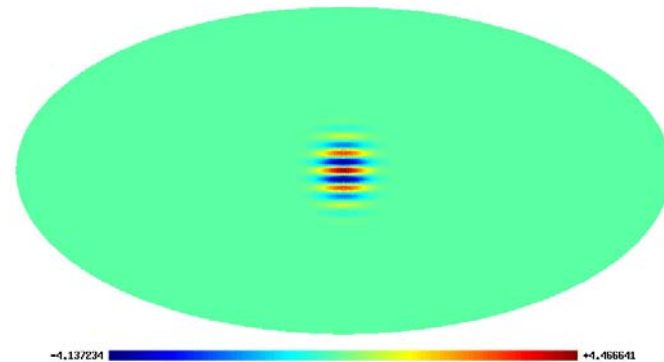
$$\psi_{S^2}(\theta, \phi) = \frac{2}{1 + \cos(\theta)} \psi_{\mathbb{R}^2}(2 \tan(\theta/2), \phi)$$

Spherical Mexhat wavelet



$$\psi_{\mathbb{R}^2}(\mathbf{x}) = \frac{1}{\sqrt{2\pi}} (1 - \|\mathbf{x}\|^2) e^{-\frac{\|\mathbf{x}\|^2}{2}}$$

Spherical real Morlet wavelet



$$\psi_{\mathbb{R}^2}(\mathbf{x}) = \cos(\mathbf{k} \cdot \mathbf{x}) e^{-\|\mathbf{x}\|^2}$$



- Continuous Spherical Wavelet Transform

$$S(a, \alpha, \beta, \gamma) = \int_{S^2} \overline{(\mathcal{R}_{\alpha, \beta, \gamma} \psi_a)(\omega')} s(\omega') d\mu(\omega')$$



Fast algorithm

- Based on fast spherical convolution of Wandelt and Gorski (2001)
- Harmonic formulation

$$S(\alpha, \beta, \gamma) = \sum_{l=0}^{l_{max}} \sum_{m=-l}^l \sum_{m'=-l}^l \left(\overline{D_{mm'}^l(\alpha, \beta, \gamma)} \psi_{lm} \right) s_{lm}$$

Wigner rotation matrix: $D_{mm'}^l(\alpha, \beta, \gamma) = e^{-im\alpha} d_{mm'}^l(\beta) e^{-im'\gamma}$

Factor rotation: $\mathcal{R}_{\alpha, \beta, \gamma} = \mathcal{R}_{\alpha - \pi/2, -\pi/2, \beta} \mathcal{R}_{0, \pi/2, \gamma + \pi/2}$

$$S(\alpha, \beta, \gamma) = \sum_{l=0}^{l_{max}} \sum_{m=-l}^l \sum_{m'=-l}^l \sum_{m''=-\min(m_{max}, l)}^{\min(m_{max}, l)} d_{m'm}^l(\pi/2) d_{m'm''}^l(\pi/2) \overline{\psi_{lm''}} s_{lm} e^{i[m(\alpha - \pi/2) + m'\beta + m''(\gamma + \pi/2)]}$$



Fast algorithm

- Discretise, interchange order of summation and shift indices

$$S[n_\alpha, n_\beta, n_\gamma] = e^{-i2\pi[n_\alpha l_{max}/N_\alpha + n_\beta l_{max}/N_\beta + n_\gamma m_{max}/N_\gamma]} \sum_{j=0}^{N_\alpha-1} \sum_{j'=0}^{N_\beta-1} \sum_{j''=0}^{N_\gamma-1} t_{j,j',j''} e^{i2\pi[jn_\alpha/N_\alpha + j'n_\beta/N_\beta + j''n_\gamma/N_\gamma]}$$

where $t_{m+l_{max}, m'+l_{max}, m''+m_{max}} = e^{i(m''-m)\pi/2}$

$$\sum_{l=\max(|m|, |m'|, |m''|)}^{l_{max}} d_{m'm}^l(\pi/2) d_{m'm''}^l(\pi/2) \overline{\psi_{lm''}} s_{lm}$$

- Evaluate $t_{j,j',j''}$ first, then use FFT to simultaneously evaluate all other summations



Algorithms

Comparison

Theoretical complexity

| Algorithm | Complexity |
|-----------|---------------------------------------|
| Direct | $\mathcal{O}(L^4 N_\gamma)$ |
| Semi-fast | $\mathcal{O}(L^3 \log_2(L) N_\gamma)$ |
| Fast | $\mathcal{O}(L^3 N_\gamma)$ |

⇒

Saving: $\mathcal{O}(L) \sim \mathcal{O}(\sqrt{N})$

Typical execution times

| N_{side} | Execution time (min:sec) | | |
|-------------------|-----------------------------|-----------|----------|
| | Direct | Semi-fast | Fast |
| 8 | 00:01.19 | 00:01.12 | 00:00.01 |
| 16 | 00:18.60 | 00:17.38 | 00:00.04 |
| 32 | 05:01.48 | 04:43.06 | 00:00.21 |
| 256 | - | - | 01:54.15 |

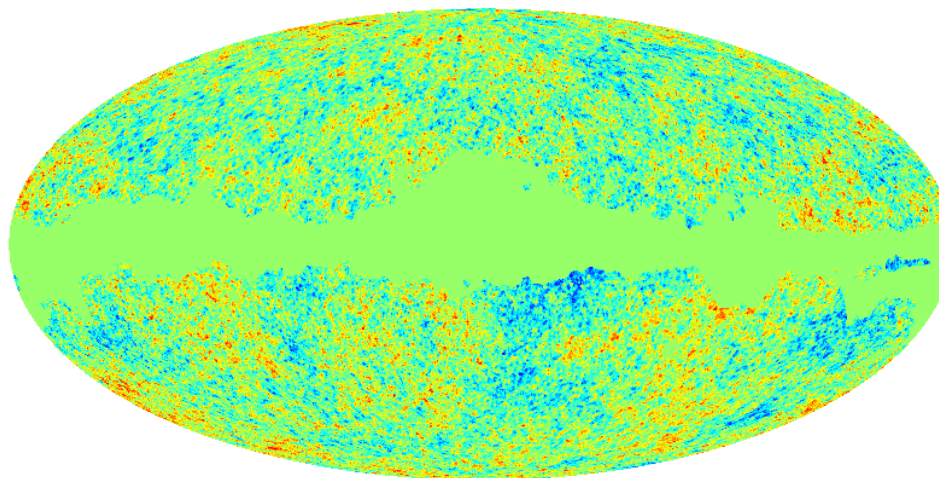
Sun Fire 280R Server

Dual UltraSPARC III 900MHz Processors

4GB Memory



- Combine foreground corrected WMAP Q-V-W bands
⇒ single signal-to-noise ratio enhanced map
- Down-sample to $N_{side}=256$ resolution
- Apply Kp0 mask to remove Galactic plane and point source contamination



-0.447622  +0.379072



- Create **Gaussian CMB realisation** from theoretical power spectrum (monopole and dipole removed)
- **Convolve** CMB realisation with each Q-V-W beam
- **Combine** simulated Q-V-W bands in same manner as WMAP data
- **Analyse** Gaussian simulated maps in same manner as WMAP data to construct Gaussian confidence regions



- Take **CSWT of data** at following scales:

| Scales | R_1 | R_2 | R_3 | R_4 | R_5 | R_6 | R_7 | R_8 | R_9 | R_{10} | R_{11} |
|--------|-------|-------|-------|-------|-------|-------|-------|-------|-------|----------|----------|
| Arcmin | 14 | 25 | 50 | 75 | 100 | 150 | 200 | 250 | 300 | 400 | 500 |

- Construct and apply extended **coefficient mask**
- Consider **statistics of wavelet coefficients** to detect deviations from Gaussianity
 - Skewness
 - Kurtosis
- Apply identical analysis to Gaussian simulated data to construct **confidence regions**

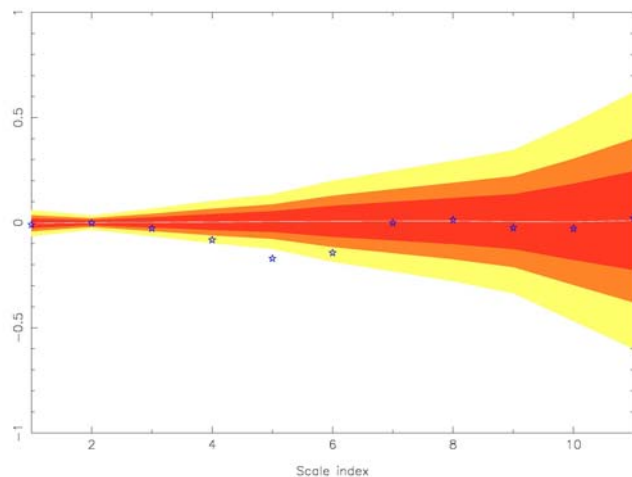


Non-Gaussianity

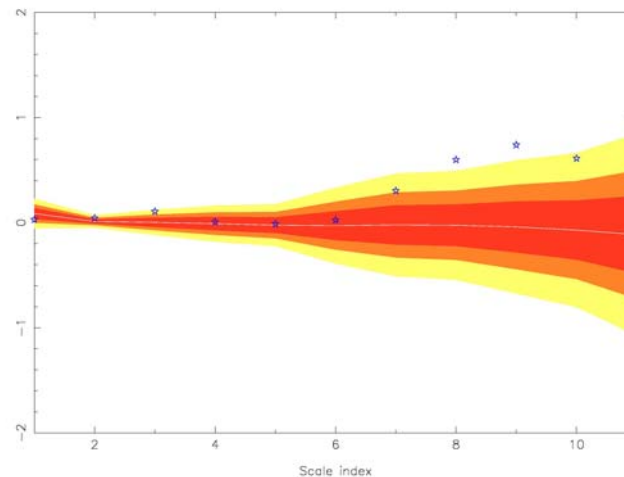
Mexhat wavelet results

- Reproduced results of Vielva et al. (2003)
- Deviation from Gaussianity detected in kurtosis at R_8 and R_9
- Possible non-Gaussianity in skewness at R_5 also detected

Skewness



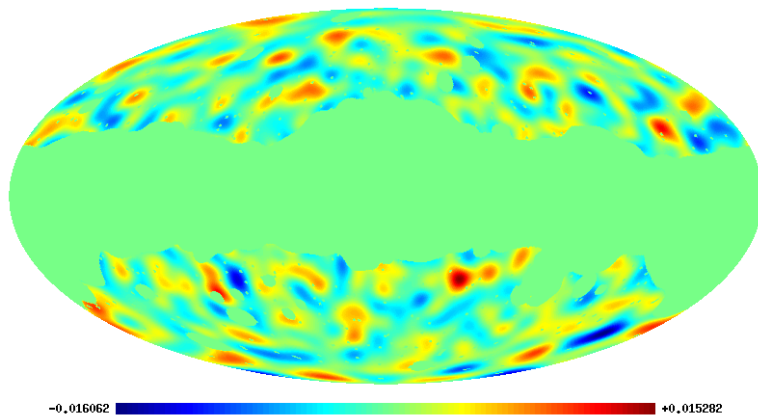
Kurtosis



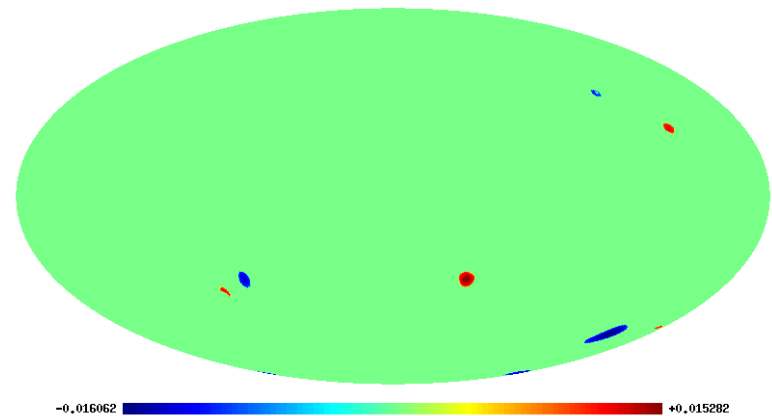
Non-Gaussianity

Mexhat wavelet results

- **Spatial localisation** of most likely deviations from Gaussianity
- Threshold R_8 coefficients below 3σ



Wavelet coefficients



Thresholded wavelet coefficients

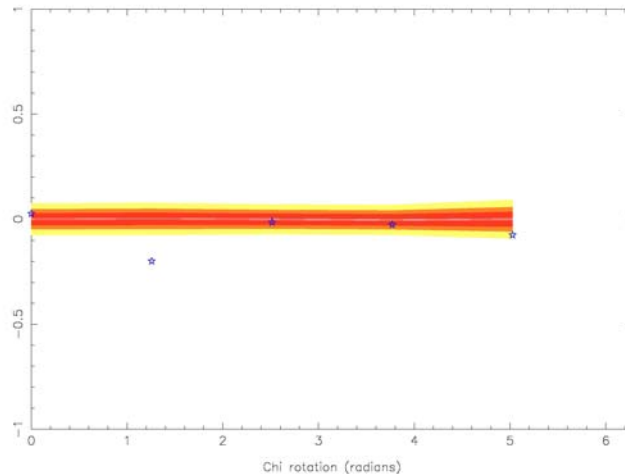


Non-Gaussianity

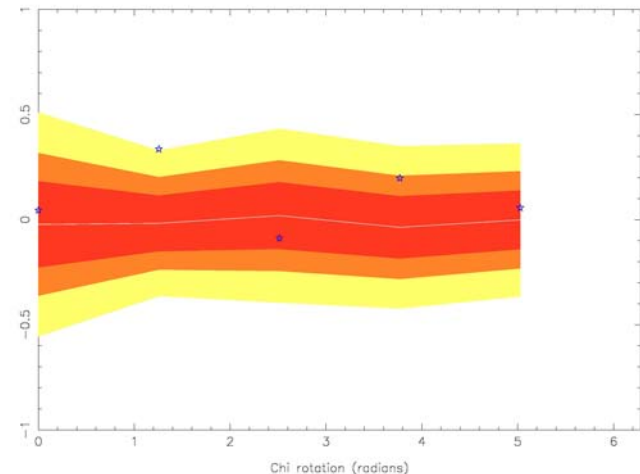
Morlet wavelet results

- Directional selectivity (consider 5 orientations)
- No significant deviations from non-Gaussianity at previous scales
- **Deviation from Gaussianity detected** at $R=750$ arcmin, $\gamma=72^\circ$

Skewness



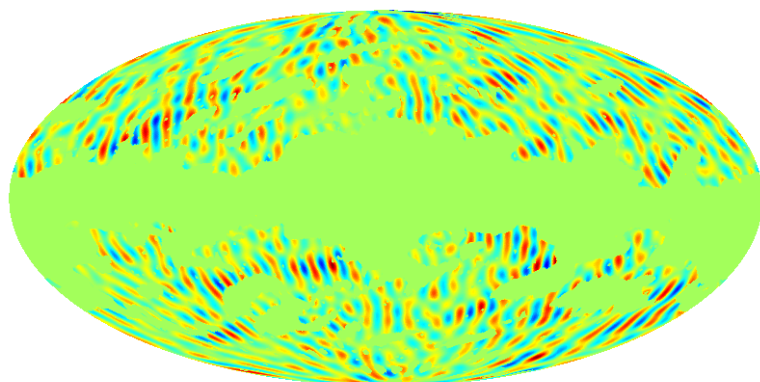
Kurtosis



Non-Gaussianity

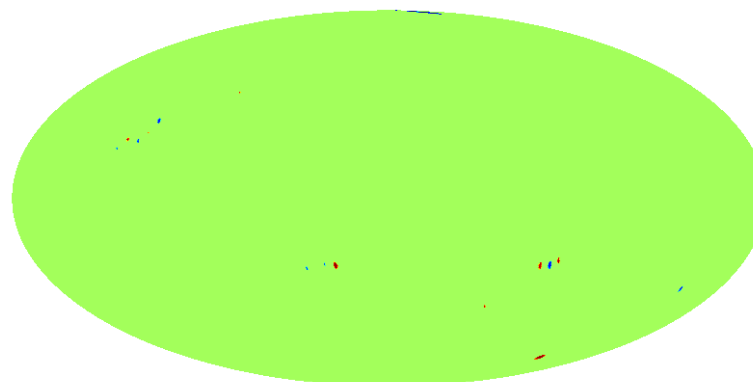
Morlet wavelet results

- Spatial and directional localisation of most likely deviations from Gaussianity
- Threshold $R=750$ arcmin, $\gamma=72^\circ$ coefficients below 3σ



-5.427E-03  +4.374E-03

Wavelet coefficients



-5.427E-03  +4.374E-03

Thresholded wavelet coefficients



Summary

- Directional Continuous Spherical Wavelet Transform
- Fast algorithms: $\mathcal{O}(L) \sim \mathcal{O}(\sqrt{N})$ saving
- Possible deviation from Gaussianity detected in WMAP
- Future work
 - Further analysis of coefficient statistics and statistical tests
 - Consider other spherical wavelets, scales, directions
 - Other applications of CSWT (e.g. compact object/defect detection using matched wavelets)
- Acknowledgements
 - Mike Hobson
 - Anthony Lasenby
 - Daniel Mortlock

